Development of Low Cost, Rapid Sampling Atmospheric Data Collection System: Part 1 – Fully Additive-Manufactured **Multi-Hole Probe**

Kyle T. Hickman*, James C. Brenner [†], Andrew Levi Ross [‡], Victoria Natalie[§] and Jamey D. Jacob[¶] Oklahoma State University, Stillwater, OK, 74078

As unmanned aircraft systems (UAS) gain more usage in acquiring remote atmospheric data, there is a need to evaluate a low-cost, high frequency multi-hole probe. Current commercially available multi-hole probes can cost up to \$5,000. This paper will evaluate the performance of 3D manufactured multi-hole probes (MHPs). The design, calibration, and validation will be explained in the paper. The calibrated probe will also serve as a wind measurement tool, part of a larger sensor payload for atmospheric measurements.

I. Nomenclature

COTSCommercial off the shelf C_{p} Coefficient of Pressure $C_{p\theta}$ Pitch Coefficient of Pressure $C_{p\phi}$ Yaw Coefficient of Pressure C_{pPitot} = Pitot Coefficient of Pressure

= Multi-Hole Probe MHPFreestream Pressure p_{∞} = Static Pressure p_a = Dynamic Pressure ReReynolds Number SLAStereo-lithography UAVUnmanned Aerial Vehicle UAS= Unmanned Aerial System

UVelocity

Freestream Velocity U_{∞} MHP Pitot Velocity $U_{PitotVelocity}$ pitot Velocity и alpha Velocity w Beta Velocity ν θ Pitch Yaw φ

Density ρ

Free stream density ρ_{∞} Dynamic Viscosity μ 3DThree Dimensional 5HPFive Hole Probe

^{*}Graduate Student; kthickm@okstate.edu, AIAA Student Member.

[†]Graduate Student; jcbrenn@okstate.edu, AIAA Student Member.

[‡]Research Engineer, Unmanned Systems Research Institute; levi.ross@okstate.edu, AIAA Student Member.

[§]Research Engineer, Unmanned Systems Research Institute; victoria.natalie@okstate.edu, AIAA Student Member.

[¶]John Hendrix Chair and Professor & Director, Unmanned Systems Research Institute; jdjacob@okstate.edu, AIAA Associate Fellow.

II. Introduction

The use of Unmanned Aerial Systems (UAS) to take meteorological measurements has been expanding in the last few decades. As the technology involved and became sophisticated so did the ability to acquire more precise and intricate data using UAV, as seen [1]. Currently there are variety of COTS (Commercial off the shelf) sensors that commonly placed on aerial platforms and used to collect meteorological data shown in the table.

Table 1 Common COTS Sensor Options

Sensor	Log Rate	Measurement
iMet XQ	10 Hz	Temperature, Pressure, Humidity GPS Lat, Long, Alt
Young 3D Ultrasonic Anemometer	32 Hz	Wind Speed and Direction
FT 2D Ultrasonic Anemometer	10 Hz	Temperature, Wind Speed, Direction
Vaisala RS92 Radiosonde	1 Hz	Temperature, Pressure, Humidity GPS Lat, Long, Alt Derived Wind Speed and Direction

As can be noted from the table, the max data log speeds, generally tend to have a maximum output rate of 10 Hz with the exception on the Young 3D Ultrasonic Anemometer but comes with the caveat of being to heavy to mount to most small UAS (2.6 lbs). These sensors also generally have a high price tag. A high data rate is required for the measurement of some atmospheric phenomena, specifically turbulence and wind gust. Accurate measurements of these would allow for better atmospheric modeling, especially in urban environments and severe weather events where the air can easily become turbulent. The main atmospheric observations that would benefit most from a higher logging rates are wind and direction. If the wind speeds could logged fast enough, then in theory one would be able to measure turbulent behavior, something that is still largely unpredictable.

A. Multi-Hole Probes

Multi-Hole probes are valuable tools for research purposes. MHPs are multi-dimensional and mean-velocities sensors that measure pressure via the set of ports on the probe tip. The head has five or more locations for pressure measurements: one on the axis of the probe and at least four at equally spaced locations around the axis. A front view of the probe head is shown in Figure 1 of a 5HP which is the configuration that will be used for this research. By comparing the pressures, it is possible to determine the pitch θ and yaw ϕ angle, and from these determine the velocity vector.

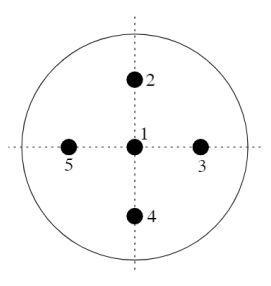


Fig. 1 Front View of Five-Hole Probe

Multi-hole probes (MHP) are currently commercially available with sensor packages that can cost upwards of thousands of dollars. The MPHs used in this study were manufactured by using an SLA 3D printer, making them easy to manufacture and cost effective. The probes are then individually calibrated in a sub-sonic wind-tunnel via a non-nulling calibration method. The probes can then be used for a wide array of research purposes.

III. Probe Design

A. Multi Hole Probe Design

As with regular manufactured MHPs, with 3D manufactured probes there are three main components of consideration for designing the probe: size, shape, and length. The tip geometries of the probe largely determines its operating characteristics. The most common tip geometries used are hemispherical, conical, and pyramid, as shown in Figure 2 from [2]. Numerous studies have demonstrated that differences in conical and pyramid tips is primarily based on performance of how flow separation behaves around the probe. One study shows that with smooth surfaces (see hemispherical or conical) separation occurs more slowly [3]. This is generally a good trait to have for MHPs, but this also comes at a cost of being sensitive to changes in Reynolds Number due to abrupt changes in the free-stream-velocity. From [4] most MHPs usually have an angular operating range of -25 degrees to 25 degrees. From previous literature studies, for the flow regions that a small UAV will be experiencing a hemispherical tip head has been shown to be the best geometry [5].

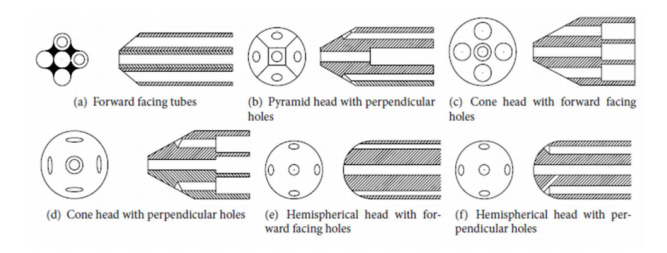


Fig. 2 5HP Tip Geometry Types[2]

B. 3D-manufactured MHP Design

Taking the knowledge from [6] studies over 5HP's, the design for the 3D-printed 5HP has a maximum outer 0.5inch diameter and hemispherical head. The maximum diameter was chosen because the diameter provided enough room for all five of the internal hole lines to be printed with the available resolution of the SLA FormLabs printer while still small enough to fit inside a small UAV and provide the performance needed based off of previous studies [6]. The inner hole diameter for the five holes probe was chosen to be 0.06 inches. This was verified to be the smallest hole diameter the SLA printer could reliably print while maintaining the integrity of the hole and keeping clear of resin debris. This diameter was also the same diameter as the pressure transducers ports on the sensor board. Each of the five holes were evenly spaced apart from each other across the 0.36 in diameters of the probe body. The static line was placed at 1.5 inches away from the tip of the probe. The static ports themselves consist of a static ring of 0.2 inches in diameter. This ring is connected by 4 perpendicular holes that extend to the outside of the probe. Then a 0.06 inch hole is connected to the static ring and runs down to the end of the probe at 2 degree offset to provide additional room at the end probe for mounting. The total length of the probe is seven inches ending in a chamfered end. The length of the probe was chosen such that it provided enough room to be safely mounted to a fixed-wing UAV or wind tunnel for testing. As the intention for this probe was to be fully 3D-printed, the pressure lines had to be able to connect to the probe itself. At the end of the probe six ports extends 0.15 inches out from the chamfered end. The end was chamfered to put each of the connecting ports at different distance to allow for easier accessibility when connecting the Tygon pressure lines to pressure ports. The probe's isometric dimensions are shown in Figure 3.

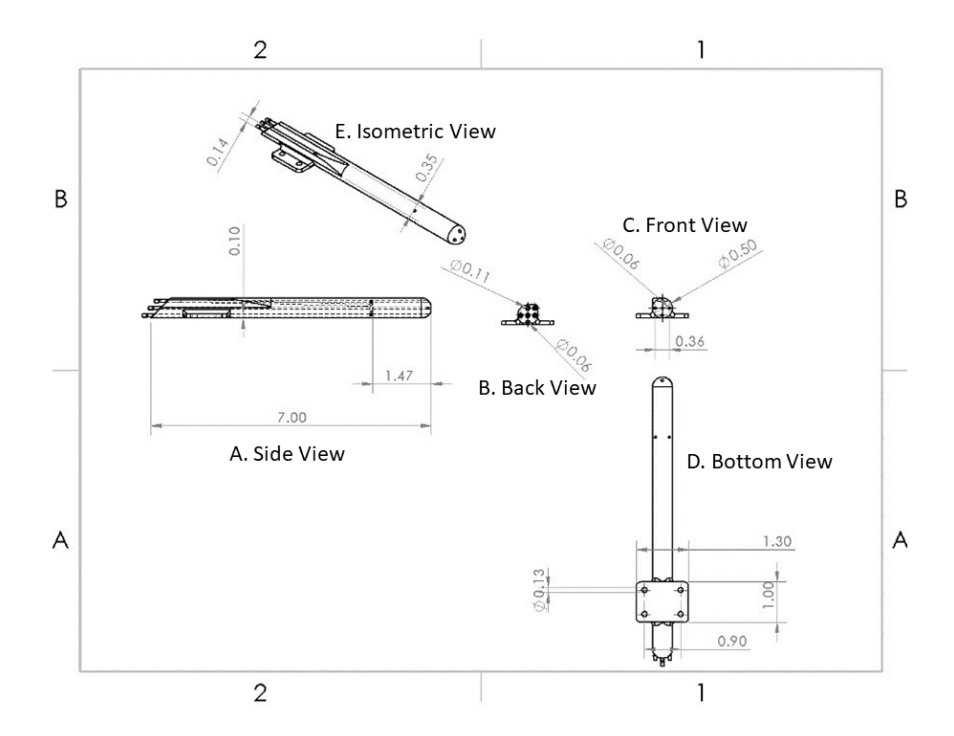


Fig. 3 Probe Dimensions: A. Side View, B. Back View, C. Front View, D. Bottom View, E. Isometric View

IV. Probe Calibration

Because of the nature of MHPs measuring 3-dimensional flow, each probe requires its own calibration[7]. This is compounded by the fact that these probes are 3d-printed and will have slightly different flow characteristics even when printed on the same 3d-printer. The goal is to determine experimentally the pressure data sets that show probe's behavior in a known flow field. Using the total and static pressures, pitch and yaw angles, and the velocity magnitudes, the data can be expressed as non-dimensional pressure coefficient values. This known flow field is taken over a range of known Reynolds numbers, Mach numbers, and velocities as the probes are traversed across a range of angles incrementally.

A. Multi-Hole Calibration Methods

The two standard methods of 5HP calibration are nulling and non-nulling (fixed-position). In a nulling calibration method, a probe is inserted into a flow and rotated until the error signal across two opposing ports (e.g alpha low and alpha high) is nulled. Then, by taking the inclination angle at that position, it is related to the flow direction, and by measuring the pressure at that position, the velocity is obtained. This method is highly accurate, but it is a very involved process that requires large amounts of space for traversing and very long data acquisition sessions. The non-nulling method calibration, while tedious, is easier to perform in a standard wind-tunnel test section. This method involves having the probe fixed in the center of the wind-tunnel and slowly rotated from one of its angular operating limits to the other, while each pressure reading of the probe is measured and correlated to the angular position of the probe. This data is then compared to a Pitot-static probe upstream in the wind-tunnel, which measures the free-stream tunnel velocity. This method was first introduced by Treastor and Yocum[8]. Due to the set up of the lab experiment available, the non-nulling method was to calibrate all of the 3d-printed probes for this research.

B. Multi-Hole Probe Calibration Equipment and Procedure

The wind-tunnel used for non-nulling calibration of the 3D manufactured probes in this experiment is a Flotech 1440 produce by GDJ Inc. with a 12X12X36 inch test section as shown in Figure 4. The wind-tunnel is equipped with a 2hp motor and capable of producing flow speeds from 0-25 m/s. The test is best suited for low Reynolds number testing and is controlled by an analog wheel that changes the RPM of the motor. The upstream Pitot-static probe that is connected to an Omega Analog sensor that outputs the pressure and velocity data through a Labview DAQ. The stepper

motor used to sweep the probe back forth is a DMX-UMD-23 stepper motor produced by ARCUS Technology. The sensor that is being used to record the pressure from the MHP is a custom made sensor board that is using a Teensy 3.6 and three digital Honeywell SSCDRRN001PD2A5 digital pressure transducers seen in Figure 5. This sensor package allows for a data capture of 200 hertz. Both pitot-static probe and the MHP were connecting to their respective sensors via Tygon tubing.



Fig. 4 Wind Tunnel Arrangement



Fig. 5 Digital Sensor Package

The procedure for the experiment started by mounting the MHP to the stepper mount via a steel rod and placing it in the center of the wind tunnel at 0 degrees as shown Figure 6. To keep the tip of the probe away from the boundary layer effects from the edges of the test chamber, the probe will pivot around its tip instead of its end. This was done by 3D-printing an extension mount that connects the probe to the steel rod.

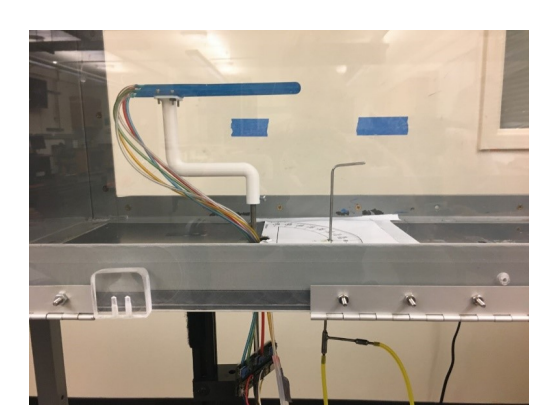


Fig. 6 MHP Mounted in Wind Tunnel

Because of the nature of the non-nulling calibration method (yawing sweeps) and 5 hole probes having pitch and yaw angular observations, only the one set of pressure holes will receive pressures differential in a given sweep. Therefore

the probes will needed to be mounted and swept in both an alpha and a beta orientation independently to properly calibrate them, as seen in Figure 7.



Fig. 7 Calibration Sweep Orientations

After the probe is mounted securely to the wind tunnel, the Tygon tubes are run through the bottom of the wind tunnel and connected to the digital sensor board. The board is then turned on by connecting the micro-USB port to a 5V power supply. Then, the wind-tunnel is turned on to a fixed speed and allowed to run continuously to reach steady-state (30 seconds). Once this is done, the stepper motor program is started and the probe moves from -45 degrees to +45 degrees in 5 degree increments. The range was chosen because the operating range for similar MHPs has been proven to be around -30 to +30 degrees. Thus the entire operating range of the probe is captured. The probe is held at each step for 30 seconds, allowing the tip flow to reach steady state and gather enough data to acquire an accurate average at that point. It is worth mentioning that the response time for the probe is much shorter than than 30 seconds (~10ms), but this allows for a more accurate calibration. The sweep is then repeated for each test cycle, and all three sweeps are averaged together for that specific speed. There are three total speeds the probes were tested at: 10, 15, and 20 m/s for both alpha orientation and beta orientation, totaling nine test per orientation. Once the experiment is performed, the data is offloaded via micro SD card, parsed in Matlab, and the graphs are generated.

C. Governing Equations

Calibration of the multi-hole probes in known flow-field and the curves associated derived from the calibrations is what makes the MHP work. The key to calibrating MHPs are the coefficient of pressures. The pressure coefficient is a non-dimensional feature that is defined by the pressure difference over the dynamic pressure. The dynamic pressure is defined as,

$$q = p_a - p_{\infty} = \frac{1}{2} * \rho_{\infty} * U_{\infty}^2$$
 (1)

For the pitch angle, this is

$$C_{p\theta} = \frac{P_2 - P_4}{P_1 - P_a} \tag{2}$$

and for the yaw angle, the equation is

$$C_{p\phi} = \frac{P_3 - P_5}{P_1 - P_a} \tag{3}$$

and for pitot coefficient of pressure

$$C_{pPitot} = \frac{U_{pitot}}{U_{\infty}} \tag{4}$$

As shown in the Figure 8 the axis being tested $C_{p\theta}$ has a slope of some gradient, whereas, $C_{p\phi}$ is nulled and has zero or nearly zero value. Another important parameter for MHP's is the angular operating range. As Figure 9. depicts, the further along the curve within the linear range gives the angular range. As mentioned before, different MHP's tip geometries affect the MHP's operating angle range. Outside of the nonlinear curve of the probe the angle sensitive is less, therefor, maintaining values of C_p that correspond to the associated angle is harder to correlate.

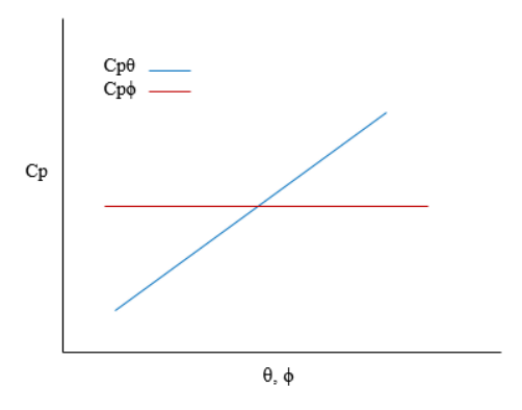


Fig. 8 Notional pressure coefficient curves for pitch and yaw depicting a 5HP traversing on the pitching axis while the yaw axis nulled

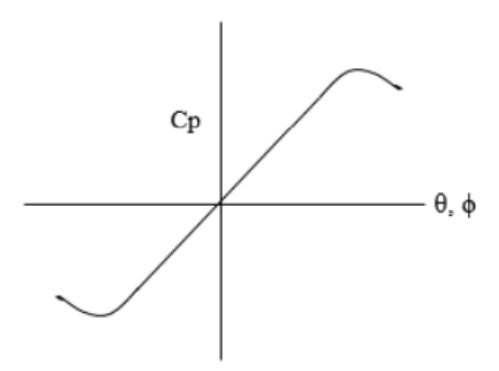


Fig. 9 Illustration depicting pressure coefficient linear range

Figure 10. shows the decomposition of velocity, U, where the rotational axis for pitch and yaw θ and ϕ are determined by from pressure differences on their respective axis using Equations 2 and 3.

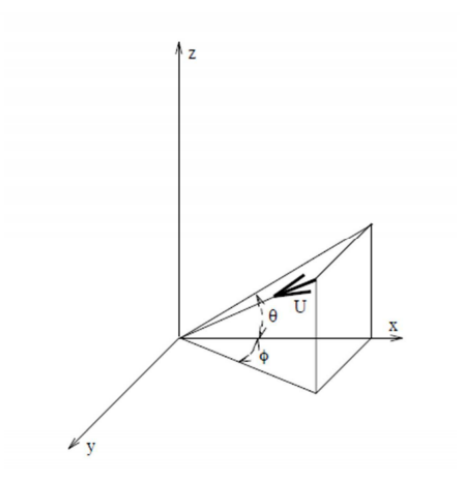


Fig. 10 Orientation of Vector pitch and yaw angle

Using the Bernoulli's equation the magnitude of the velocity vector can be resolved.

$$U = \sqrt{\frac{2}{\rho_{\infty}}q} = \sqrt{\frac{2}{\rho_{\infty}}(p_o - p_{\infty})}$$
 (5)

Fig. 11 shows a ideal velocity magnitude curve with symmetry about about θ and ϕ . As the probe is symmetric, the curve should ideally be symmetric about θ and ϕ .

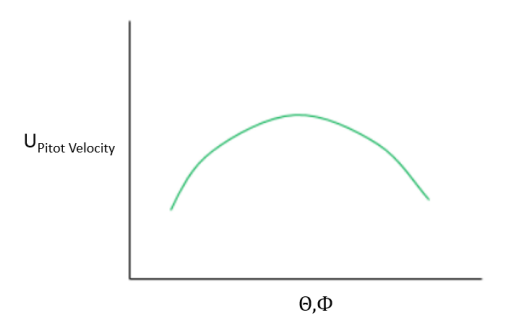


Fig. 11 Ideal Velocity Magnitude Curve

After calculating the magnitude and obtaining the direction of the velocity, the three velocity components can be be calculated by using equations ??, 8, and 7.

$$Re = \rho * u * L/u \tag{6}$$

$$w = U\sin(\phi) \tag{7}$$

$$v = Usin(\theta)cos(\phi) \tag{8}$$

D. Revnolds Number

The main measurement gain from using MHP is velocity, the effect of Reynolds number should be considered for calibration [9]. Increasing the know flow-field velocity of the wind tunnel will increase the Reynolds regime as well to its relationship to velocity.

$$Re = \frac{\rho * U_{\infty} * D}{u} \tag{9}$$

During the calibrations a range of Reynolds number should be set. The range of the Reynolds number is dependent on the expected operating range of the MHP. For these MHP's that operating range is the flight regime of the UAVs it being is mounted to (10 - 25 m/s). With that being stated multiple speeds of the flight regime should be tested to ensure the consistent of the MHP calibration. For these probes speeds of 10, 15, and 20 m/s were chosen.

V. Calibration and Validation

The results presented in this section are obtained from the experimental and methodology previously discussed. The goal of these results are to demonstrate the accuracy and the repeatably of the 3D-manufactured probe design.

A. Calibration of Probes

Calibration results for the 3D-manufactured probes are presented below for both the pressure coefficient and velocity magnitude curves.

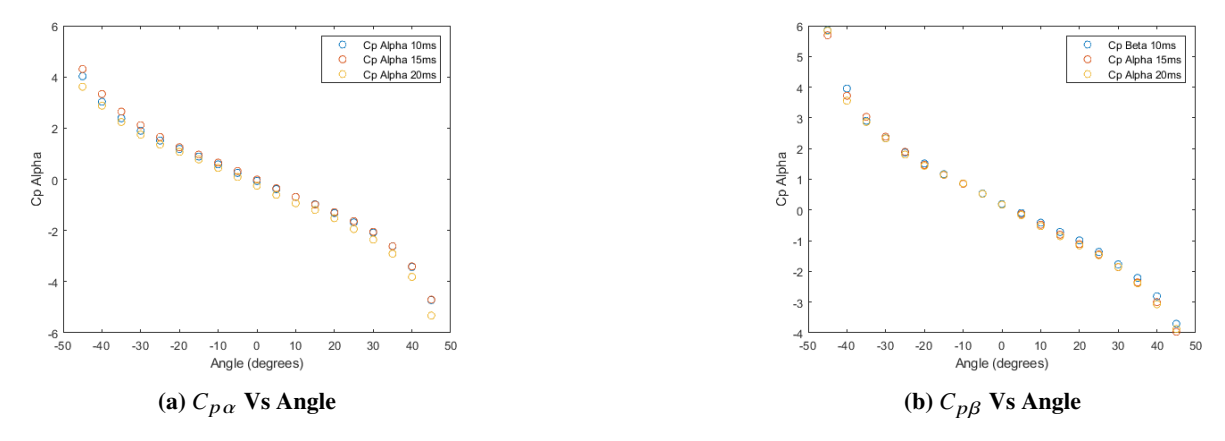


Fig. 12 Probe2 (a) C_p Alpha Vs. Angle and (b) C_p Beta Vs Angle

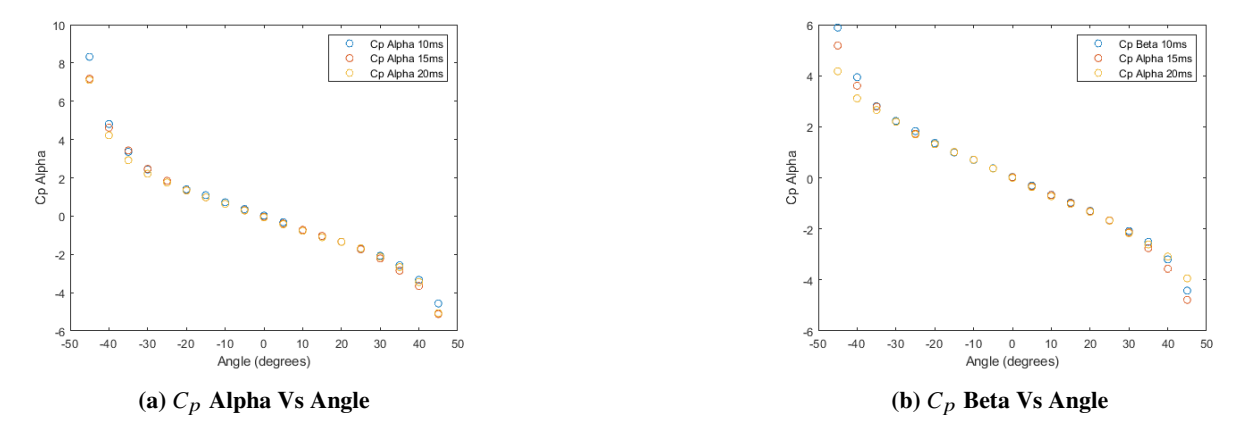
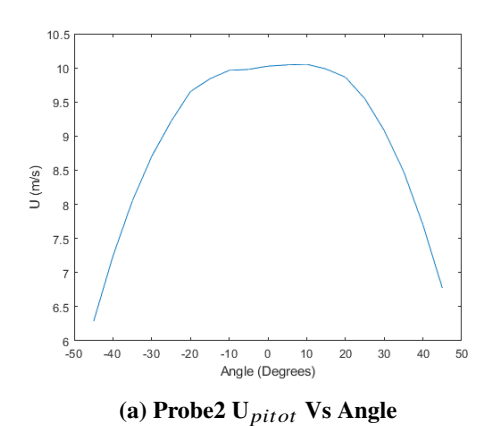


Fig. 13 Probe3 (a) C_p Alpha Vs. Angle and (b) C_p Beta Vs Angle

Note the linear range of the Probe2 falls offs significantly at the outer ranges of the MHP (45 and -45). This confirms past research in that it shows the probes performance is not adequate at these angle ranges and therefor should only be operated in angles within its linear range of (30 to -30) degrees. Figure 12 also shows the similarity of C_p values across all three speeds tested. The linear relationship for both probes has a R^2 value of 0.95 (almost 1) indicating there is a good overall data fit. The Probe3 results are shown in Figure 13. The comparison between the two probes demonstrates the repeat-ability of the probe design.



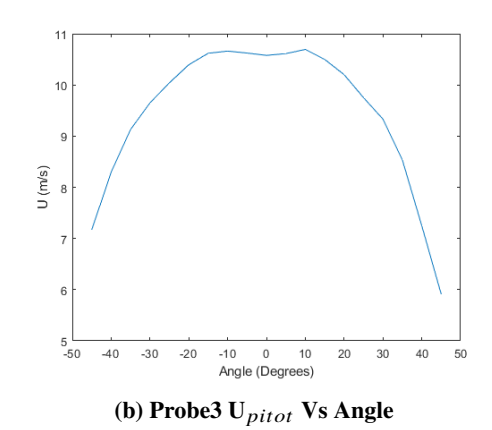


Fig. 14 Magnitude Pitot Velocity Vs Angle

Figure 14 show the magnitude velocity curve for the 3D-manufactured probes. The figures show symmetry of the maximum velocities throughout the traverse from -45 to $+45^{\circ}$ demonstrating the repeat-ability of the 3D-manufactured probes

B. Interpolation From Unknown Data

After proper calibration of the probes the calibration data can be tabled and used to interpolate velocities and angles from unknown measurements. Development of the 3D-manufactured probe is done with the intended use on UAS fixed winged vehicles in mind. The intended vehicles mostly stay under 40 m/s as the flight speed. This allows for the interpolation process for probe to be simplified since the probe will stay in a laminar flow for the duration of measurements. This is significant because the three major quantities used for interpolation, $C_{p\alpha}$, $C_{p\beta}$, and C_{ppitot} will not have significant changes over the expected air speeds.

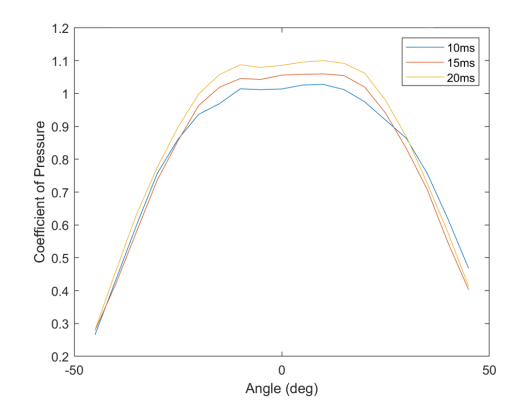


Fig. 15 $C_{p \, pitot}$ Change with Velocity and Angle

Figure 15 illustrates how C_{ppitot} changes from 10 to 20 m/s. The C_{ppitot} trends for each or the three speeds are nearly identical. For interpolation purposes the assumption that no significant change between speed was made. This same assumption was made for $C_{p\alpha}$ and $C_{p\beta}$ these trends are graphed in Figure 12b. These assumptions allow for the interpolation process to be broken down into five major steps.

- 1) Calculate $C_{p\beta}$ and $C_{p\alpha}$ from the pressure measurements.
- 2) Interpolate for Alpha and Beta from the coefficient of pressures.
- 3) Use Alpha and Beta to interpolate for C_{ppitot}
- 4) Use C_{ppitot} to Calculate U using Equation 4
- 5) Using Equations ??, 8, and 7 with Alpha as ψ and Beta as θ resolve the velocity vectors.

As a step to verify that the interpolation method works the code was used to resolve angles and velocities from calibration data. The calibration data provides a good known quantity for to test the interpolations against. The values that are compared are the values of Alpha and Beta, and the velocities(total and components).

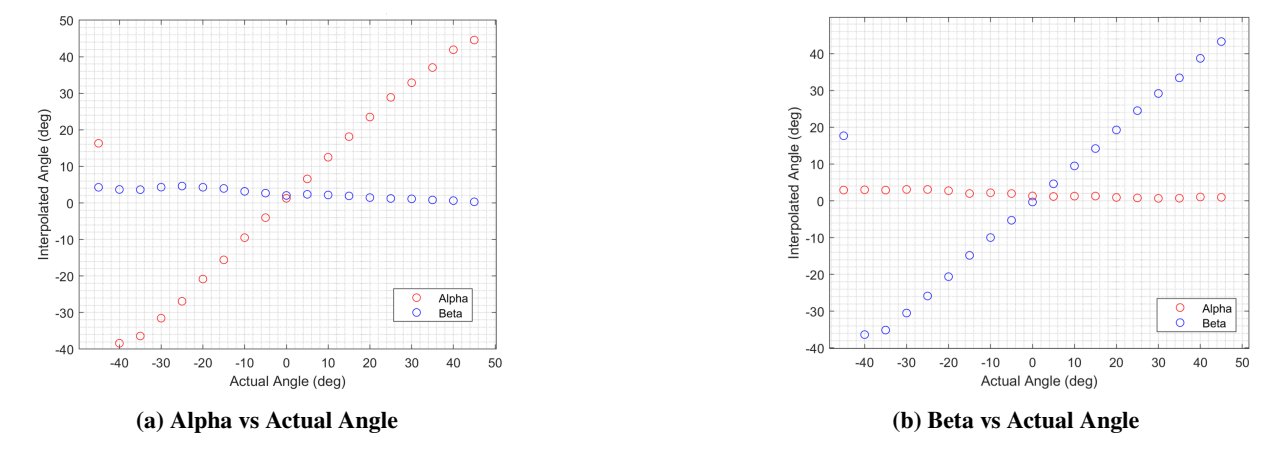


Fig. 16 Probe3 Interpolated Comparison to Actual Angle

Figure 16 is a comparison between the known Alpha and Beta angles and the interpolated values. One major outlier is present. The -45° angle has a significant error. This is constant across all three probes and all test. The cause for this error is currently unknown. More test will be done to attempt to isolate the cause of the error. However, the error should be outside the conditions encounter by a fixed wing UAS and should not affect normal data operations.

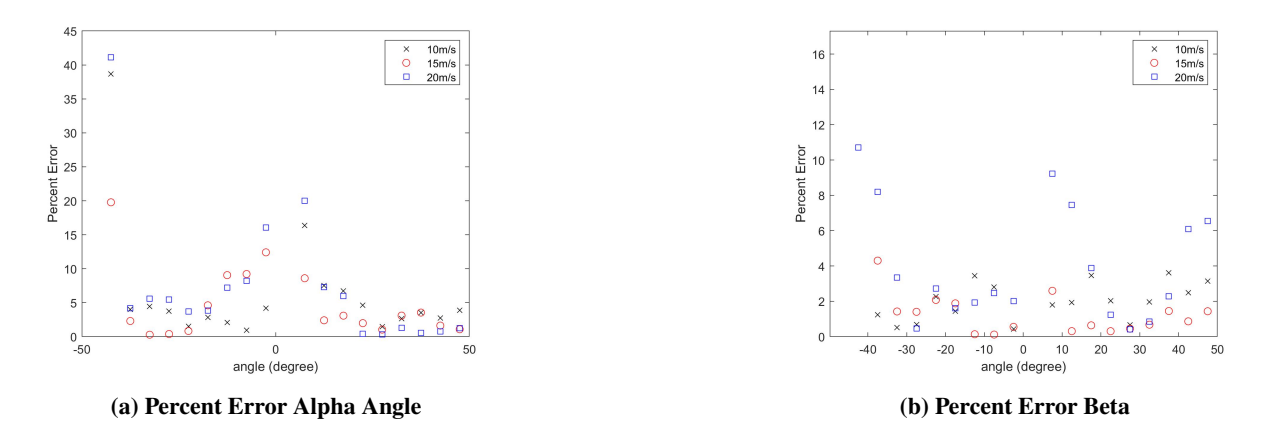


Fig. 17 Percent Error of Interpolated Angles

Figure 17 shows the percent error for the different angle interpolations across the three different speeds. Note the for the graphs the -45° percent error was near 100. For scaling purposes it was removed from the graph. There is a peak around the 0° . One of the causes of this could be asymmetry in the probe tip that is unexpected causing pressure differentials. The second interpolation point to verify is the velocities.

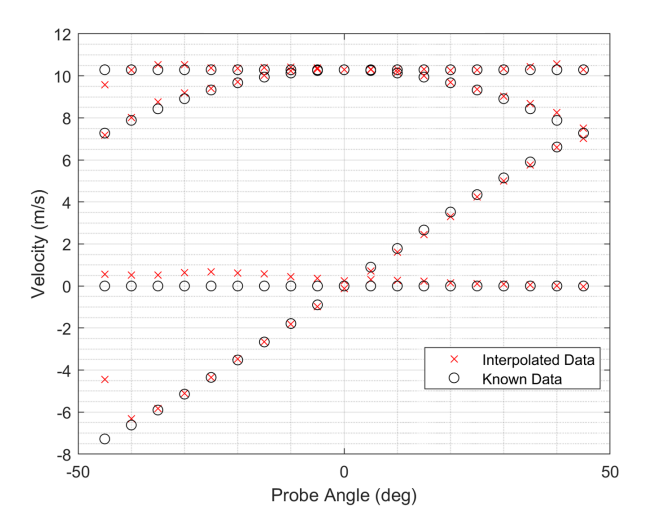


Fig. 18 Velocity Comparison for 10m/s Alpha Sweep

Figure 18 shows a comparison between the known velocities and the interpolated velocities for a 10 m/s alpha sweep. As previously noted there is still an anomaly at the -45° step. Other than that issue the interpolated data is relatively accurate.

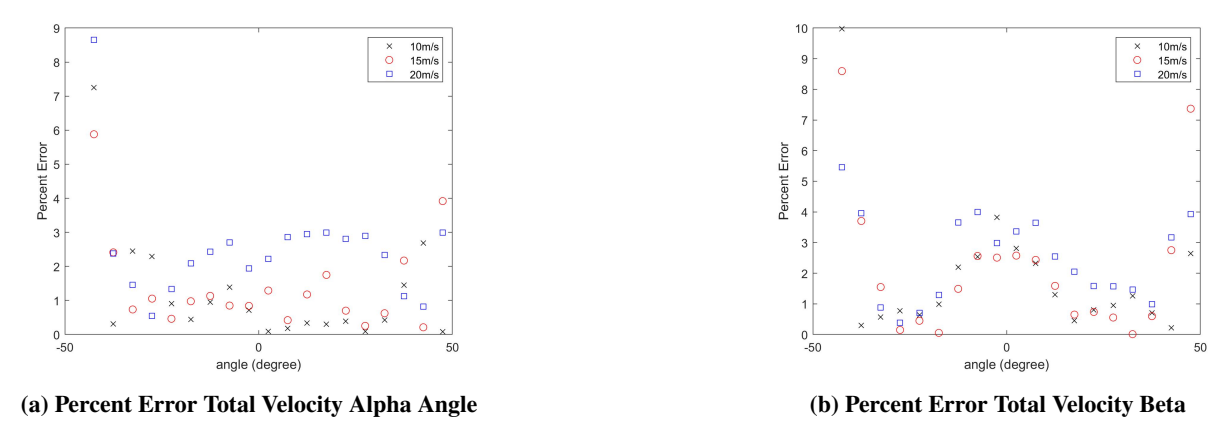


Fig. 19 Percent Error of Interpolated Angles

Figure 19 is the percent error of the Total velocity interpolations. The errors stay relatively low except for at the 45° extremes. The percent error also increases with velocity. The error increase near zero degrees in the Beta orientation exist the same as it did with the angles. Overall the Beta error has a is less linear. This could be due to print support defects left on the probe. Due to the print method small bumps of support material are left along the side of the probe. While these are sanded they may still cause pressure disturbances along the probe.

C. Preliminary Flight Data



Fig. 20 5HP Mounted to VTOL Nimbus

Once the probes were calibrated, they are mounted to inside the nose cone of a VTOL nimbus as shown in Figure 20. Preliminary flight testing was conducted at the Oklahoma State University flight field on 6-23-2020.

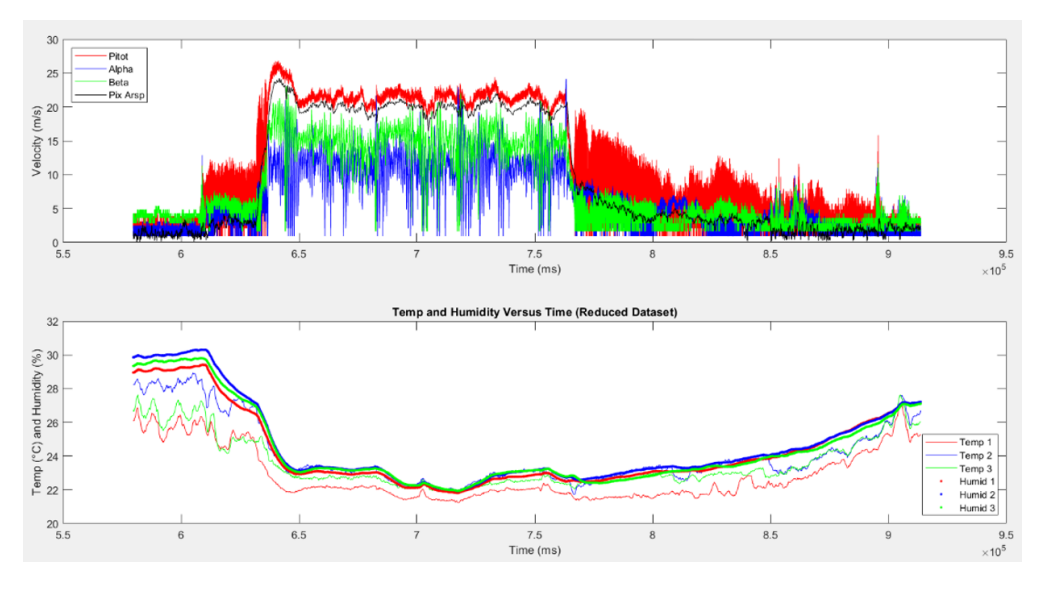


Fig. 21 Preliminary Flight Test 5HP vs Pixhawk

Below in Figure 21 the top graph shows the MHP-Pitot velocity and the Pixhawk airspeed. The MHP velocity matches up very well to the Pixhawk airspeed data. The graph also shows MHP velocity has a faster reaction time then Pixhawk, because of the high refresh rate of the sensor, making it ideal for measuring wind and turbulence. The bottom graph show the alpha and beta velocities alongside the pitot velocity. The alpha and beta values are much smaller then the pitot, as they should because of the forward flight of the aircraft. The true values of these velocities were not known from the flight test, but this is a good indication that the MHP is working correctly. More flight testing is required to validate the MHP values in the field. For more information on the flight test and the UAV sensor package see [10].

VI. Conclusion and Future Work

In conclusion, the result of this paper demonstrate an accurate and low-cost 3D-manufactured 5HP that can be used for a multitude of research purposes. The paper shows the 3D manufactured 5HP performs very well to commercial-off-the-shelf (COTS) 5HPs and other multi-hole probes. For future work more flight tests will be conducted to verify the 5HP interpolations and velocities performance in a unknown flight field. Additionally, the 5HP will be

compared to ultrasonic anemometers as cheaper alternative to be used with UAV for weather research. A novel method of doing a wake survey with the 5HP's will also be tested and used to verify the accuracy of the probes. The full system is detailed in a partner paper [10].

Acknowledgments

This work is supported in part by the National Science Foundation under Grant No. 1539070, *Collaboration Leading Operational UAS Development for Meteorology and Atmospheric Physics (CLOUD-MAP)*, and Grant No. 1925147, *NRI: Safe Wind-Aware Navigation for Collaborative Autonomous Aircraft in Low Altitude Airspace*, and by NASA under the University Leadership Initiative. Additional support provided by the OSU Unmanned Systems Research Institute. We appreciate the assistance of many USRI staff and students.

References

- [1] Martin, S., Bange, J., and Beyrich, F., "Meteorological profiling of the lower troposphere using the research UAV "M2AV Carolo."," *Atmos. Meas. Tech. Discuss*, Vol. 3, No. 6, 2010, pp. 5179–5209.
- [2] Donnell, G. W., Feight, J. A., Lannan, N., and Jacob, J. D., "Wind characterization using onboard IMU of sUAS," 2018 Atmospheric Flight Mechanics Conference, 2018, p. 2986.
- [3] Telionis, Y., D. Yang, and Rediniotis, O., "Recent developments in multi-hole probe (mhp) technology," *International Congress of Mechanical Engineering*, 2009.
- [4] Sitaram, N., and Srikanth, K., "Effect of chamfer angle on the calibration curves of the five hole probes," *International Journal of Rotating Machinery*, 2014.
- [5] Zeiger, M., Chalmeta, L., and Telionis, D., "Tip geometry effects on calibration and performance of seven-hole probes," *29th AIAA, Fluid Dynamics Conference*, 1998, p. 2810.
- [6] Azertash-Namin, S. K., "Evaluation of Low-Cost Multi-Hole Probes for Atmospheric Boundary Layer Investigation," *Masters Thesis, Oklahoma State University*, 2017.
- [7] Huffman, G. D., Rabe, D., and Poti, N., "Flow direction probes from a theoretical and experimental point of view," *Journal of Physics E: Scientific Instruments*, Vol. 13, No. 7, 1980, p. 751.
- [8] Treaster, A. L., and Yocum, A. M., "The Calibration and Application of Five-Hole Probes," *ISA transactions*, 1979. https://doi.org/10.21236/ada055870.
- [9] Dudzinski, T. J., and Krause, L. N., Flow-direction measurement with fixed-position probes, National Aeronautics and Space Administration, 1969.
- [10] Ross, L., Natalie, V., Brenner, J., Hickman, K., and Jacob, J., "Development of Low Cost, Rapid Sampling Atmospheric Data Collection System: Part 2, Complete Package," *Sci-Tech* 2021, 2021.